



Published in final edited form as:

Chem Commun (Camb). 2015 October 7; 51(78): 14624–14627. doi:10.1039/c5cc06325f.

Fluorescent Mimics of Cholesterol that Rapidly Bind Surfaces of Living Mammalian Cells

David Hymel, Sutang Cai, Qi Sun, Rebecca S. Henkhaus, Chamani Perera, and Blake R. Peterson

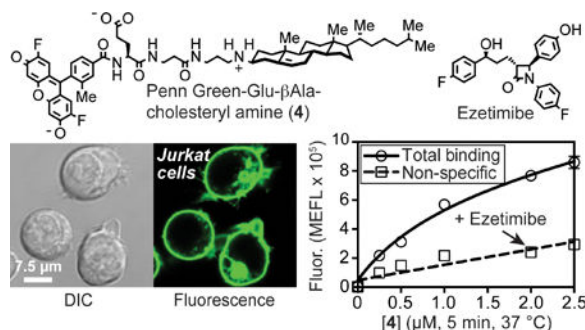
The University of Kansas, Department of Medicinal Chemistry, Lawrence, KS 66045

Blake R. Peterson: brpeters@ku.edu

Abstract

Mammalian cells acquire cholesterol, a critical membrane constituent, through multiple mechanisms. We synthesized mimics of cholesterol, fluorescent *N*-alkyl-3 β -cholesterylamine-glutamic acids, that are rapidly incorporated into cellular plasma membranes compared with analogous cholesteryl amides, ethers, esters, carbamates, and a sitosterol analogue. This process was inhibited by ezetimibe, indicating a receptor-mediated uptake pathway.

Abstract



Cholesterol (**1**) is a critical constituent of membranes of mammalian cells. Cells acquire exogenous forms of this sterol through multiple mechanisms involving structurally distinct cell surface receptors. Lipoprotein particles such as low-density lipoprotein (LDL) and high-density lipoprotein (HDL) carry cholesteryl esters (**2**) and associated protein and lipid components throughout the bloodstream.¹ Cells expressing LDL and HDL receptors actively internalize these natural nanoparticles via receptor-mediated endocytosis. In contrast, Niemann-Pick C1 Like 1 protein (NPC1L1) plays key roles in the cellular uptake of dietary (unesterified) cholesterol (**1**), as found in mixed micelles.² This receptor was identified in 2004³ as a target of ezetimibe (**3**), a drug used to treat hypercholesterolemia. More recent

Correspondence to: Blake R. Peterson, brpeters@ku.edu.

[†]Electronic Supplementary Information (ESI) available: Experimental details, characterization data, and additional figures. See DOI: 10.1039/x0xx00000x

studies suggest that although NPC1L1 is a primary target of ezetimibe and its active glucuronide metabolite,⁴⁻⁶ other proteins, such as the HDL receptor SR-BI, can also be inhibited by this drug.⁷ Recent proteomics experiments have identified over 250 cholesterol-binding proteins, including receptors, channels, and enzymes.⁸

Derivatives of cholesterol have numerous biological applications. These compounds have been used to facilitate the delivery of small inhibitory RNA (siRNA),⁹ enhance DNA transfection,¹⁰ probe cellular membrane subdomains,¹¹ and assay cholesterol transport processes.¹²⁻¹⁷ Cholesteryl carbamates have been extensively investigated, and cellular uptake of cholesteryl carbamate-conjugated siRNA has been reported to be similar to uptake of cholesteryl esters, requiring binding to HDL or LDL,⁹ followed by internalization via HDL or LDL receptors. This initial lipoprotein-binding step can slow cellular uptake, and the presence of high concentrations of serum (e.g. 10%) in media typically reduces the activity of these compounds, likely because of competition between serum lipoproteins and cognate cell surface receptors.

In an effort to mimic the molecular recognition properties of free cholesterol (**1**), we hypothesized that the protonated secondary amino group of *N*-alkyl-3 β -cholesterylamines,^{18, 19} as found in compounds **4-7**, might function as a bioisostere for the 3 β -hydroxyl group of cholesterol. Thus, in contrast to cholesteryl esters, cholesteryl carbamates, and structurally related compounds, which may require lipoprotein-mediated cellular uptake, these compounds might bind to receptors on cell surfaces that recognize free cholesterol or structurally similar metabolites through alternative mechanisms. We further hypothesized that the addition of anionic amino acids might affect binding to serum proteins and increase the affinity of these compounds for cells.

To investigate how structural features affect recognition of cholesterol derivatives and related compounds by proteins on the surface of cells, we synthesized the fluorescent molecular probes **4-13**. For probes derived from 3 β -cholesterylamine, this steroid building block,²⁰ and some cholesterylamine-derived intermediates,²¹ were prepared as previously reported. The novel building block 3 β -sitosterylamine was prepared from sitosterol using methodology described for the synthesis of 3 β -cholesterylamine.²⁰ The 4-carboxy Pennsylvania Green fluorophore was prepared as previously described.²² Full synthetic details are provided in Scheme S1 and Scheme S2 of the supporting information. These probes were designed to systematically compare membrane anchors derived from *N*-alkyl-3 β -cholesterylamines (**4-7**), a sitosteryl analogue (**8**), a *N*-acyl-3 β -cholesterylamine (**10**), or cholesterol (**9**, **11-13**) linked to the hydrophobic Pennsylvania Green^{23, 24} (PG) fluorophore through amino acid subunits. We hypothesized that the carbonyl linked to the steroid in amide **10**, ester **11** or carbamates **12** and **13** would be similar to natural cholesteryl esters, and this structural modification might correspondingly affect their ability to bind cell surfaces.

As shown in Figure 1, confocal laser scanning microscopy was employed to compare living human Jurkat lymphocyte cells after treatment with **4-13**. These experiments demonstrated that a brief (5 minute) treatment of cells with **4** or **5** (2 μ M) at 37 °C results in robust fluorescent staining of cellular plasma membranes. Examination of these cells after 1 hour showed enhanced cellular binding, uptake of the probe, and localization in transferrin-

positive early/recycling endosomes (Figure 1 and Figure S1 of the supporting information). Binding of **4** (and **5**) to cell surfaces was predominantly receptor-mediated as evidenced by up to 80% inhibition upon coaddition with excess (200 μ M) ezetimibe (**3**, Compare Figure 1A and 1C, and see Figure S3 of the supporting information). This inhibition indicates that proteins on cell surfaces may recognize these compounds as mimics of free cholesterol or related cholesterol metabolites. These metabolites might include structurally related cholesterol sulfate²⁵ and cholesterol glucuronide,²⁶ which are present in micromolar concentrations in the bloodstream of animals. Comparison of **4** with **6** lacking the glutamic acid residue in the linker region revealed that the anionic moiety of **4** is critical for rapid high affinity/efficacy binding to cells (Figure 1, compare panels B and G). Moreover, despite the presence of a structurally analogous glutamic acid, the cholesteryl carbamate **12** showed low cellular binding and cellular uptake compared with **4**, supporting the hypothesis that carbamates engage a mechanistically distinct cellular uptake pathway. However, this loss of activity of **12** could be at least partially rescued by addition of a second glutamic acid, as found in **13**.

Using ezetimibe (**3**, 200 μ M, 0.2% DMSO) as a specific competitor, we quantified the relative affinities (K_d , app) and efficacies (B_{max}) of rapid binding of **4-13** to Jurkat lymphocytes in media containing 10% serum. Data from saturation binding experiments after treatment for five minutes, designed to limit cellular uptake by endocytosis, are shown in Figure 2, Table 1, and the supporting information. The high affinity and efficacy of binding of **4** and **5** to cell surfaces compared to **6-12** revealed that *N*-alkyl cholesteryl amines bearing an anionic functional group and a spacer residue such as β -alanine most efficiently bind cell surfaces, a critical initial step for initiation of endocytosis and delivery of linked agents. The absence of substantial cellular binding of the sitosterolamine analogue (**8**), differing from **4** by the presence of an additional ethyl group in the tail of the sterol, further supports a specific receptor-mediated uptake mechanism. This result is consistent with limited receptor-mediated^{27, 28} uptake of phytosterols such as sitosterol by mammalian cells.

To investigate whether other cell types show differential effects, we examined rapid (5 min) binding of **4**, **5**, **8**, and **13** to three different human cell lines. Human Jurkat cells, grown in suspension were compared with the human cell lines HeLa and HEK-293, which were suspended in media prior to treatment. As shown in Figure 3, HeLa cells bound the fluorescent cholesterol mimics to the greatest extent. Comparison of HeLa with Jurkat and HEK-293 cells revealed 3.3-fold to 8.1-fold more specific binding to HeLa cell surfaces compared to the other cell lines. These results might be explained by higher expression by HeLa cells of a specific receptor that interacts with these compounds.

For these assays, cellular fluorescence was converted to molecules of equivalent fluorescein (MEFL) using fluorescent bead standards. For the Jurkat cell line, this analysis indicated that treatment with **4** or **5** at a concentration of 2 μ M for 5 minutes loads $0.5-1.5 \times 10^6$ molecules into the plasma membrane of individual cells. This rapid and massive increase in cellular fluorescence suggested that an enzyme may be actively inserting these compounds into the cellular plasma membrane. Further analysis of time-dependent fluorescence resulting from treatment with **4**, **5**, **8**, and **13** using the Michaelis-Menten model of enzyme kinetics is shown in Figure 4. These studies revealed that the cellular uptake of **4**, **5**, and to a lesser

extent **13**, is highly efficient, with $1.8\text{--}5.0 \times 10^5$ molecules incorporated per minute per cell, consistent with a catalytic process. Kinetic values of K_M and V_{\max} from this analysis are shown in Table 1.

In conclusion, we identified novel structure-activity relationships that govern binding of fluorescent cholesterol mimics to the surface of living mammalian cells. New cholesterol-mimetic membrane anchor motifs of **4**, **5**, and **13** were identified that engage a rapid cellular uptake pathway, consistent with a receptor-mediated process, that catalytically inserts these compounds into the plasma membrane. Although the receptor or enzyme targeted by these compounds has not yet been identified, it is unlikely to be NPC1L1, the classical pharmacological target of ezetimibe, because this protein is not highly expressed outside of the liver and intestine,²⁹ and the active metabolite ezetimibe-glucuronide, prepared as previously reported,³⁰ does not inhibit binding of **4** to Jurkat cell surfaces (data shown in Figure S2 of the supporting information). Given that cholesterol trafficking and distribution involves dynamic receptor-mediated and vesicular processes that are not completely understood,³¹ these compounds have potential as novel probes and tools for the delivery of impermeable molecules into mammalian cells.

Supplementary Material

Refer to Web version on PubMed Central for supplementary material.

Acknowledgments

This work was supported by the National Institutes of Health (R01-CA83831 and P20-GM103638) and the University of Kansas Cancer Center.

References

1. Goldstein JL, Brown MS. *Arterioscler Thromb Vasc Biol.* 2009; 29:431–438. [PubMed: 19299327]
2. Wang LJ, Song BL. *Biochim Biophys Acta.* 2012; 1821:964–972. [PubMed: 22480541]
3. Altmann SW, Davis HR Jr, Zhu LJ, Yao X, Hoos LM, Tetzloff G, Iyer SP, Maguire M, Golovko A, Zeng M, Wang L, Murgolo N, Graziano MP. *Science.* 2004; 303:1201–1204. [PubMed: 14976318]
4. Weinglass AB, Kohler M, Schulte U, Liu J, Nketiah EO, Thomas A, Schmalhofer W, Williams B, Bildl W, McMasters DR, Dai K, Beers L, McCann ME, Kaczorowski GJ, Garcia ML. *Proc Natl Acad Sci USA.* 2008; 105:11140–11145. [PubMed: 18682566]
5. Ge L, Wang J, Qi W, Miao HH, Cao J, Qu YX, Li BL, Song BL. *Cell Metab.* 2008; 7:508–519. [PubMed: 18522832]
6. Garcia-Calvo M, Lisnock J, Bull HG, Hawes BE, Burnett DA, Braun MP, Crona JH, Davis HR Jr, Dean DC, Detmers PA, Graziano MP, Hughes M, Macintyre DE, Ogawa A, O'Neill K A, Iyer SP, Shevell DE, Smith MM, Tang YS, Makarewicz AM, Ujjainwalla F, Altmann SW, Chapman KT, Thornberry NA. *Proc Natl Acad Sci USA.* 2005; 102:8132–8137. [PubMed: 15928087]
7. Labonte ED, Howles PN, Granholm NA, Rojas JC, Davies JP, Ioannou YA, Hui DY. *Biochim Biophys Acta.* 2007; 1771:1132–1139. [PubMed: 17442616]
8. Hulce JJ, Cognetta AB, Niphakis MJ, Tully SE, Cravatt BF. *Nat Methods.* 2013; 10:259–264. [PubMed: 23396283]
9. Wolfrum C, Shi S, Jayaprakash KN, Jayaraman M, Wang G, Pandey RK, Rajeev KG, Nakayama T, Charrise K, Ndungo EM, Zimmermann T, Koteliansky V, Manoharan M, Stoffel M. *Nat Biotechnol.* 2007; 25:1149–1157. [PubMed: 17873866]

10. Pitard B, Oudrhiri N, Vigneron JP, Hauchecorne M, Aguerre O, Toury R, Airiau M, Ramasawmy R, Scherman D, Crouzet J, Lehn JM, Lehn P. *Proc Natl Acad Sci USA*. 1999; 96:2621–2626. [PubMed: 10077560]
11. Sato SB, Ishii K, Makino A, Iwabuchi K, Yamaji-Hasegawa A, Senoh Y, Nagaoka I, Sakuraba H, Kobayashi T. *J Biol Chem*. 2004; 279:23790–23796. [PubMed: 15026415]
12. Zhang J, Cai S, Peterson BR, Kris-Etherton PM, Heuvel JP. *Assay Drug Dev Tech*. 2011; 9:136–146.
13. Wustner D. *Chem Phys Lipids*. 2007; 146:1–25. [PubMed: 17241621]
14. Wustner D, Solanko L, Sokol E, Garvik O, Li ZG, Bittman R, Korte T, Herrmann A. *Chem Phys Lipids*. 2011; 164:221–235. [PubMed: 21291873]
15. Maxfield FR, Wustner D. *Methods Cell Biol*. 2012; 108:367–393. [PubMed: 22325611]
16. Holtta-Vuori M, Uronen RL, Repakova J, Salonen E, Vattulainen I, Panula P, Li ZG, Bittman R, Ikonen E. *Traffic*. 2008; 9:1839–1849. [PubMed: 18647169]
17. Sankaranarayanan S, Kellner-Weibel G, de la Llera-Moya M, Phillips MC, Asztalos BF, Bittman R, Rothblat GH. *J Lipid Res*. 2011; 52:2332–2340. [PubMed: 21957199]
18. Peterson BR. *Org Biomol Chem*. 2005; 3:3607–3612. [PubMed: 16211095]
19. Hymel D, Peterson BR. *Adv Drug Deliv Rev*. 2012; 64:797–810. [PubMed: 22401875]
20. Sun Q, Cai S, Peterson BR. *Org Lett*. 2009; 11:567–570. [PubMed: 19115840]
21. Sun Q, Cai S, Peterson BR. *J Am Chem Soc*. 2008; 130:10064–10065. [PubMed: 18613675]
22. Woydziak ZR, Fu L, Peterson BR. *Synthesis-Stuttgart*. 2014; 46:158–164. [PubMed: 24914246]
23. Mottram LF, Maddox E, Schwab M, Beaufilets F, Peterson BR. *Org Lett*. 2007; 9:3741–3744. [PubMed: 17705395]
24. Mottram LF, Boonyarattanakalin S, Kovel RE, Peterson BR. *Org Lett*. 2006; 8:581–584. [PubMed: 16468716]
25. Strott CA, Higashi Y. *J Lipid Res*. 2003; 44:1268–1278. [PubMed: 12730293]
26. Wade AP. *Clin Chim Acta*. 1970; 27:109–116. [PubMed: 5412592]
27. Gould RG, Jones RJ, LeRoy GV, Wissler RW, Taylor CB. *Metabolism*. 1969; 18:652–662. [PubMed: 5799288]
28. Wang LJ, Song BL. *Biochim Biophys Acta*. 2012; 1821:964–972. [PubMed: 22480541]
29. Davis HR Jr, Altmann SW. *Biochim Biophys Acta*. 2009; 1791:679–683. [PubMed: 19272334]
30. Kvaerno L, Ritter T, Werder M, Hauser H, Carreira EM. *Angew Chem Int Ed Engl*. 2004; 43:4653–4656. [PubMed: 15352196]
31. Iaea DB, Maxfield FR. *Essays Biochem*. 2015; 57:43–55. [PubMed: 25658343]

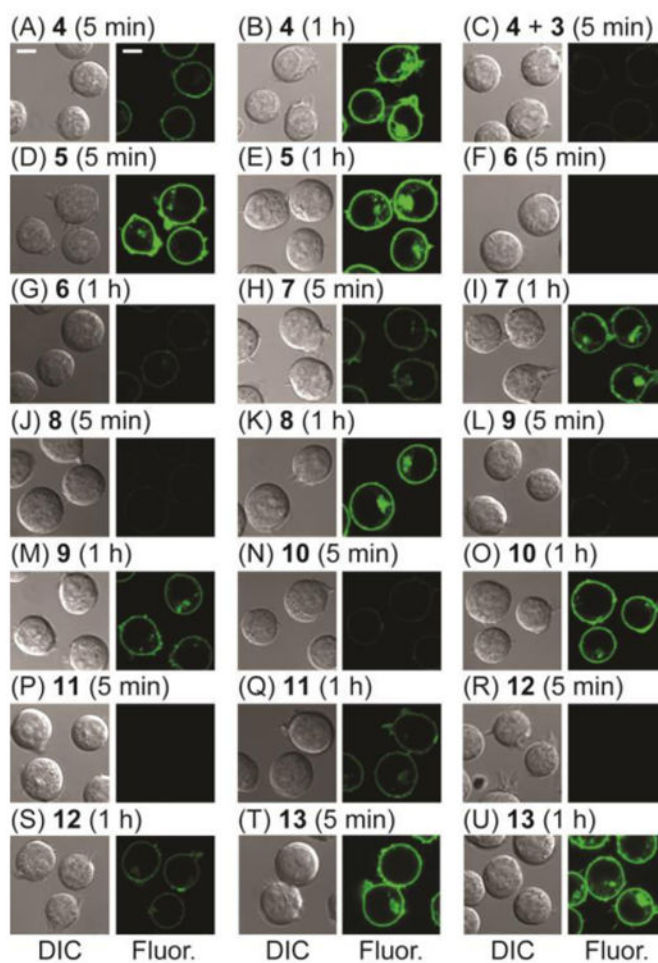


Fig. 1. Differential interference contrast (DIC) and confocal laser scanning microscopy of living Jurkat lymphocytes in media containing 10% serum. Cells were treated with fluorescent compounds **4–13** (2 μ M) at 37 $^{\circ}$ C for 5 min or 1 h. In panel C, ezetimibe (**3**, 200 μ M in 0.2% DMSO) was included to illustrate competitive inhibition of uptake of **4**. Scale bar = 7.5 microns.

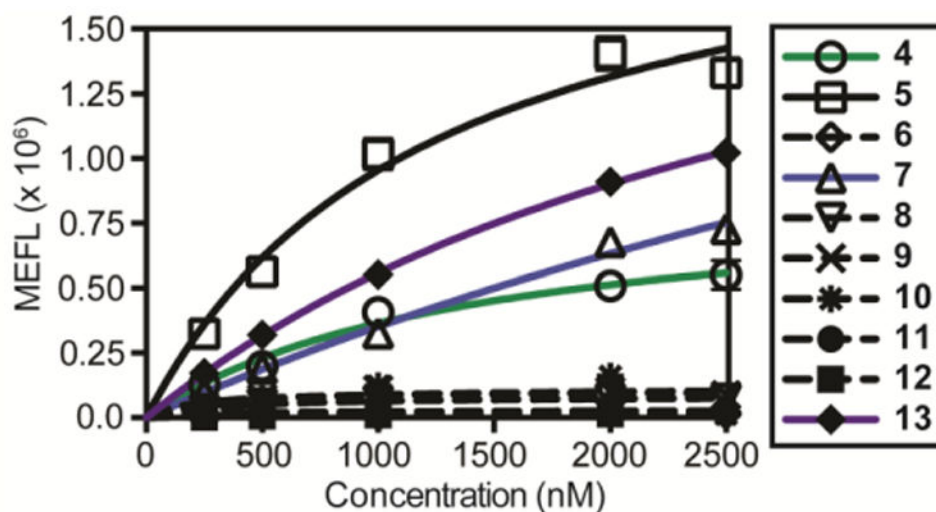
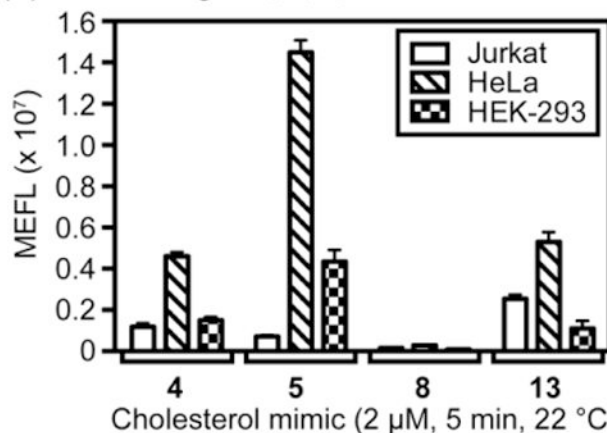
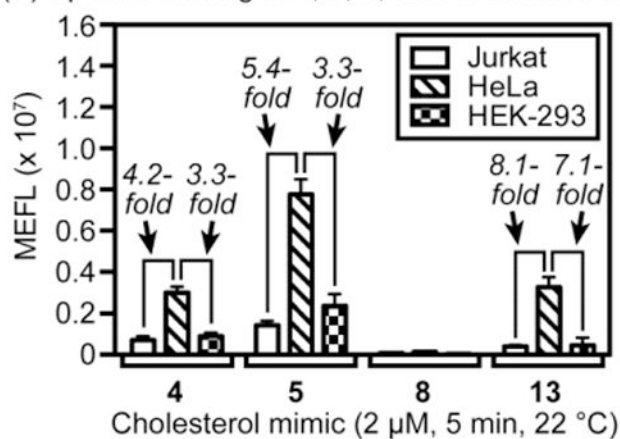


Fig. 2. Specific binding of compounds **4–13** to plasma membranes of living Jurkat lymphocytes in media containing 10% serum. Cells were treated with **4–13** for 5 min at 37 °C and analyzed by flow cytometry with and without excess ezetimibe (**3**, 200 μ M) in saturation binding experiments. The linear non-specific binding component was subtracted from the total binding data followed by curve fitting with a one-site binding model (GraphPad Prism 6).

(A) Total binding of **4**, **5**, **8**, and **13** to three cell lines(B) Specific binding of **4**, **5**, **8**, and **13** to three cell lines**Fig. 3.**

Total binding (A) and specific binding (B) of compounds **4**, **5**, **8**, and **13** to three mammalian cell lines. Cells in media containing 10% serum were treated with compounds, without (A) and with (B) excess ezetimibe (**3**, 200 μ M), in triplicate at 22 $^{\circ}$ C for 5 min. Jurkat, HeLa, and HEK-293 cells were suspended in media prior to treatment and analysis of fluorescence by flow cytometry.

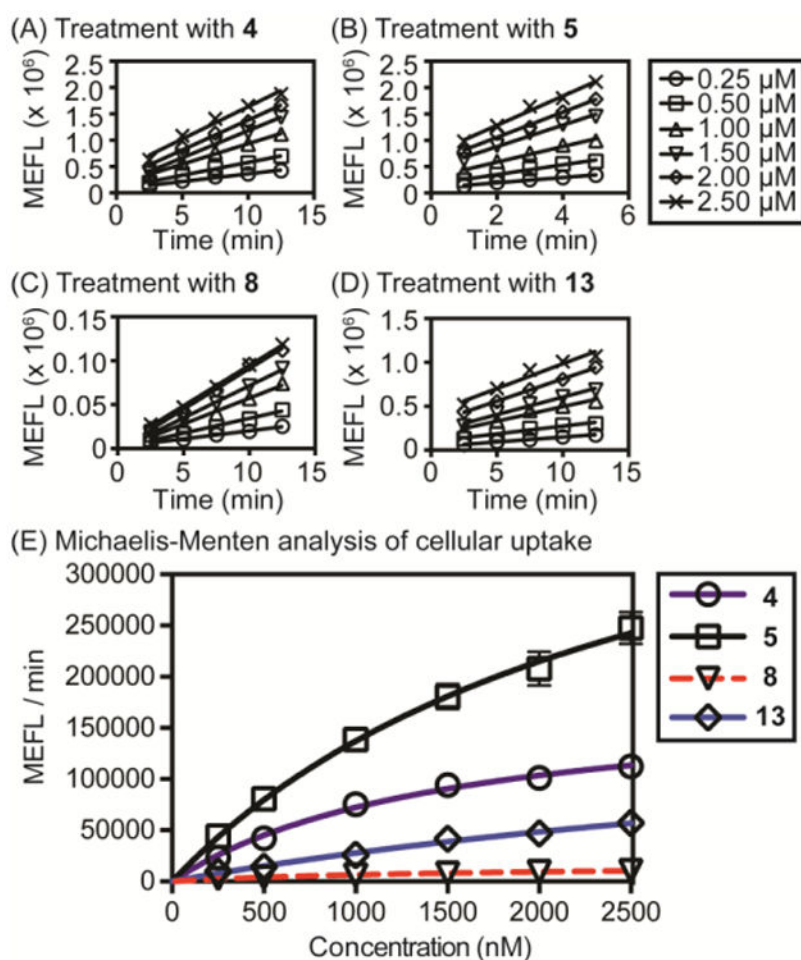
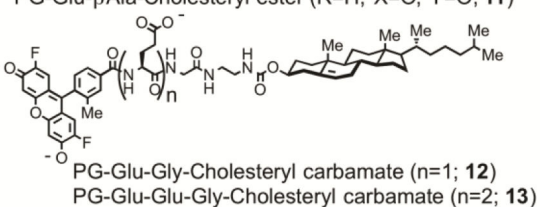
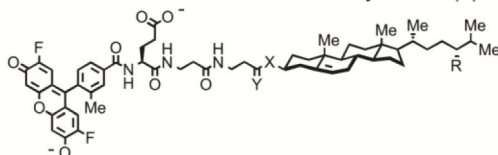
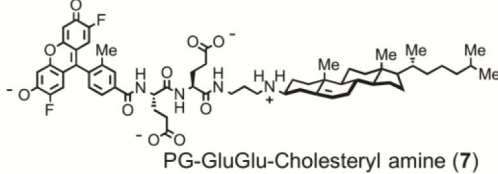
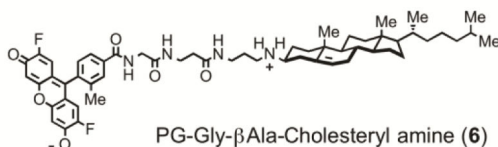
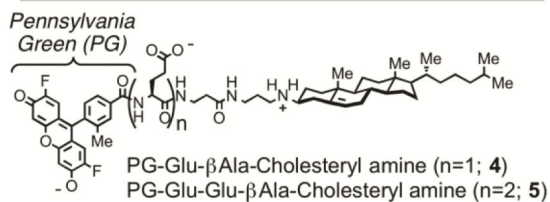
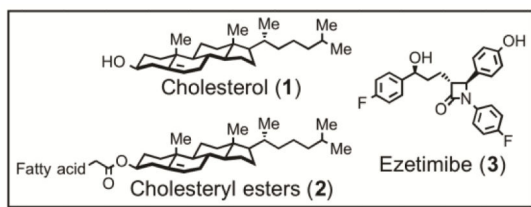


Fig. 4. Analysis of the kinetics of cellular uptake of compounds **4**, **5**, **8**, and **13**. Panels A-D: Living Jurkat lymphocytes in media containing 10% serum were treated with compounds in triplicate at 22 °C, aliquots were sampled at the times shown and fluorescence analyzed by flow cytometry. Panel E: Values of MEFL/min, obtained by linear regression of the data shown in A-D, was analyzed with a Michaelis-Menten model (GraphPad Prism 6).



Unnumbered Figure.

Table 1

Left columns: Apparent affinity ($K_{d, app}$) and efficacy (B_{max}) of binding of **4–13** to plasma membranes of living Jurkat cells. Cells were treated with compounds at 37 °C for 5 min in media containing 10% FBS (\pm SEM). Non-specific binding was quantified with ezetimibe (200 μ M) as a competitor; vehicle = 0.2% DMSO; NC: Not calculated due to low efficacy. Right columns: Values of K_M and V_{max} calculated from Michaelis-Menten analysis of rapid time-dependent cellular uptake at 22 °C (Figure 3). ND: Not determined. MEFL: molecules of equivalent fluorescein. Data, based on measurements in triplicate, is reported as mean \pm SEM.

Compd.	$K_{d, app}$ (μ M)	B_{max} (MEFL $\times 10^6$)	K_M (μ M)	V_{max} (MEFL / min $\times 10^5$)
4	1.4 \pm 0.5	0.9 \pm 0.1	1.5 \pm 0.3	1.8 \pm 0.2
5	1.2 \pm 0.2	2.1 \pm 0.2	2.6 \pm 0.7	5.0 \pm 0.8
6	NC	NC	ND	ND
7	7.7 \pm 4.1	3.1 \pm 1.3	ND	ND
8	NC	NC	1.8 \pm 0.5	0.2 \pm 0.1
9	NC	NC	ND	ND
10	NC	NC	ND	ND
11	NC	NC	ND	ND
12	NC	NC	ND	ND
13	3.2 \pm 0.6	2.34 \pm 0.28	5.8 \pm 2.2	1.9 \pm 0.5